Surface-Initiated Grafting of Dendritic Polyglycerol from Mussel-Inspired Adhesion-Layers for the Creation of Cell-Repelling Coatings

Michaël W. Kulka,* Chuanxiong Nie, Philip Nickl, Yannic Kerkhoff, Arushi Garg, Dirk Salz, Jörg Radnik, Ingo Grunwald, and Rainer Haag*

Biofouling is a major challenge in the application of textiles, biosensors, and biomedical implants. In the current work, a straightforward method for the solvent-free polymerization of antifouling dendritic polyglycerol (dPG) from mussel-inspired dendritic polyglycerol (MI-dPG) coatings on hydrophilic titanium dioxide (TiO_2) and hydrophobic polydimethylsiloxane (PDMS) is reported. Surface characterization is performed by static water contact angle (CA) measurements, X-ray photoelectron spectroscopy (XPS), and scanning electron microscopy (SEM). Significant lower CA values are obtained after dPG grafting from MI-dPG-coated TiO_2 and MI-dPG coated PDMS. Furthermore, XPS shows a time-dependent increase of the C—O bond content upon dPG grafting from MI-dPG-coated TiO_2 and MI-dPG-coated PDMS. Analysis of the surface morphology by SEM shows a clear time-dependent increase in the surface roughness upon dPG grafting from MI-dPG-coated TiO_2 and MI-dPG-coated PDMS. When the viability of two adhesive cell types is studied via LIVE/DEAD staining, a strong reduction in the cell density is observed after the dPG grafting from MI-dPG-coated TiO_2 and MI-dPG-coated PDMS (a decrease of >95% in all cases). The combined results show that biocompatible but highly cell-repelling surfaces are efficiently constructed via the grafting of dPG from MI-dPG-coated TiO_2 and MI-dPG-coated PDMS.

1. Introduction

Unspecific biofouling is a considerable challenge in the application of medical implants, biosensors, and other surgical and protective equipment in hospitals.[1] For example, biofouling can lead to deterioration of the surface, and increases the risk of infectious contamination and thrombosis (e.g., in case of joint prosthesis, urinary catheters, and intravenous stents).[2]

Furthermore, biofouling is encountered in marine applications, where it is the cause of high expenses resulting from fouling-related decreased fuel efficiency.[3] Additionally, the metabolic activity of the attached organisms can cause local corrosion, thus creating further costs.[4] Many projects have focused on the development of long-term stable nonfouling surface coatings for industrial-, marine-, and biomedical-applications. The immobilization of hydrophilic polymeric substances has proven itself as an effective strategy for the introduction of antifouling surface properties.[5] The mechanism underlying the fouling-resistance of hydrophilic polymer coatings is based on the formation of a surface hydration layer in the absence of net charge. This hydration layer acts as a physical barrier for the prevention of unspecific protein-fouling, and furthermore prevents cellular- and bacterial-adhesion.

Many methods for the surface-immobilization of polymeric substances have been developed, including but not limited to: the use of polymeric layer-by-layer assemblies,[6] irradiation-mediated grafting,[7] Langmuir–Blodgett deposition,[8] and the use of electrostatic or hydrophobic adsorption.[9] Additionally, thiol- and silane-chemistry are classically used for the functionalization of noble metals and hydroxylated surfaces, respectively.[10] Although these methods can be applied to a wide variety of substrates, most of these processes require complex machinery and/or specific

Dr. M. W. Kulka, C. Nie, P. Nickl, Y. Kerkhoff, A. Garg, Prof. R. Haag
Institute for Chemistry and Biochemistry
Freie Universität Berlin
Takustraße 3, Berlin 14195, Germany
E-mail: michaelkulka91@gmail.com; haag@chemie.fu-berlin.de

P. Nickl, Dr. J. Radnik
BAM – Federal Institute for Material Research and Testing
Division of Surface Analysis and Interfacial Chemistry
Unter den Eichen 44–46, Berlin 12205, Germany

Dr. D. Salz, Prof. I. Grunwald
Fraunhofer Institute for Manufacturing Technology
and Advanced Materials IFAM
Wiener Straße 12, Bremen 28359, Germany

Prof. I. Grunwald
Hochschule Bremen – City University of Applied Sciences
Department of Industrial and Environmental Biology
Neustadtswall 30, Bremen 28199, Germany

**ADVANCED
SCIENCE NEWS**

www.advancedsciencenews.com

**ADVANCED
MATERIALS
INTERFACES**

www.advmatinterfaces.de

chemical or physical properties of the support material, thus limiting their application. Therefore, there is a need for the development of straight-forward surface-functionalization procedures, for the facile functionalization of a wide range of substrate-types. An interesting alternative for the immobilization of polymeric substances is the use of mussel-inspired surface chemistry. Mussels can rapidly adhere to virtually every type of organic or inorganic surface under wet conditions, even to substrates that are classically categorized as adhesion resistant (e.g., polytetrafluoroethylene (PTFE)).[11] Mussels adhere themselves to the surface via an adhesive plaque that is excreted by the mussels' foot at the end of the byssal threads.[12] Earlier works showed the high prevalence of the catechol-containing amino acid L-DOPA and the amine-containing amino acid L-lysine in the mussel foot proteins (Mfps) that are excreted close to the substrate (i.e., mainly Mfp-5).[12] Based on these findings, Waite and Tanzer hypothesized the essence of the catechol moieties in the substrate-independent binding character of some of the Mfps.[13] Later works confirmed the adhesion of catechols to a broad range of substrates via the formation of hydrogen-bonds, via $\pi-\pi$ stacking, via the formation of coordination complex structures, and via the formation of Michael adducts and Schiff bases under oxidizing conditions.[14] The reversible surface binding of the catechols via the formation of complex structures was found to be especially strong in case of titanium dioxide (TiO_2) substrates, with a single molecule interaction force of ≈ 800 pN.[15]

In 2007, Messersmith and co-workers hypothesized that the high prevalence of amine and catechol functional groups in the Mfps could contribute to the rapid adhesion of mussels.[16] Therefore, dopamine was selected as a small molecule containing both amine and catechol functionalities. When dopamine-containing solutions were buffered to a basic pH, auto-oxidation of the catechol moieties to their respective *o*-quinone forms occurred. Subsequently, a series of polymerizing reactions occurred, which finally led to the formation of polydopamine (PDA) coatings on a wide variety of substrates. The PDA coating was easily postfunctionalized with amine- or thiol- containing secondary reagents via straightforward dip coating procedures, introducing specific surface properties. As a result of its substrate-independent applicability and facile postfunctionalization, the PDA coating has gained a lot of interest in the field of biomaterials, e.g., PDA has been applied in bone and tissue engineering, for the introduction of antimicrobial activity to the surface, in the creation of surfaces with patterned cell adhesion, and for the introduction of anticoagulant surface properties.[17] Although PDA has proven itself as a useful tool for surface functionalization, the initial coating procedure suffered from slow polymerization rates and a limited coating thickness.[16] Additionally, resulting from its dark-brown to black color, the PDA coatings is unsuitable for various optical applications.[16] Various methods for the acceleration of the polymerization reaction of PDA have been developed, but most of these methods utilize toxic agents to enhance the polymerization rate.[18] Therefore, there is a further need for the development of substrate-independent coating materials for the introduction of tailored surface properties.

In 2014, Wei et al. developed mussel-inspired polyglycerol (MI-dPG), which did not only contain the functional groups that are commonly found in Mfps, but also mimicked the molecular structure and weight of Mfps (**Figure 1**).[19] Polymerization of MI-dPG under slightly basic conditions led to the

rapid formation of substrate-independent coatings with a controllable coating roughness and thickness (up till 4 µm after 4 h of coating).[19] Furthermore, the coatings appeared transparent at low coating thickness. Earlier works by our group have shown the facile postfunctionalization of the MI-dPG coating with nanoparticles and amine-containing secondary reagents, for the introduction of antifouling and antibacterial surface properties.[20] Furthermore, the amine moieties of the MI-dPG coating have been utilized for the immobilization of acyl chloride-containing secondary reagents.[21]

In the current scientific literature, the immobilization of poly(ethylene glycol) (PEG) is often considered as the gold standard for the creation of antifouling surface coatings.[22] For instance, in Messersmith's initial work on PDA, cell-repelling surface properties were introduced to the surface via the covalent grafting of thiol- or amine-terminated methoxy-PEG (mPEG) onto PDA coatings.[16] Unfortunately, PEG suffers from issues considering instability upon heating in air,[23] and immunological recognition upon repeated exposure.[24] Therefore, there is a need for the development of hydrophilic antifouling surface coatings that show similar or better antifouling properties than PEG, while showing higher biocompatibility and oxidative/thermal stability than PEG under physiological conditions. The use of polyglycerol (PG) offers an interesting alternative for the creation of antifouling coatings. An earlier work by our group showed that MI-dPG coatings that are functionalized with linear polyglycerol show better antifouling properties and higher stability than similar PEG-functionalized MI-dPG coatings.[25] Furthermore, Siegers and coworkers showed the higher oxidative stability of bulk dendritic polyglycerol (dPG) in comparison to PEG.[26] Additionally, multiple projects have shown that the immobilization of dPG on the substrate is an effective strategy for the creation of antifouling surfaces.[26,27] Although these approaches clearly illustrated the antifouling potency of PG, most of them required multistep functionalization of the PG molecule prior to surface functionalization, thus leading to high production costs. Khan et al. and Moore et al. gave alternative approaches that both grafted dPG directly from silica (Si)-based substrates.[28] However, both approaches required the use of the highly reactive caustic base sodium methoxide.[28] A method reported by Weber et al. showed the grafting of dPG from aluminum, steel, and silicon surfaces without the use of a base. However, the grafting reactions were performed in an organic solvent, and the substrates required the introduction of –OH moieties to the surface prior to the grafting process.[29] In the current work, the surface-bound amines of the MI-dPG coating were utilized to initiate ring-opening polymerization of bulk glycidol (i.e., in a solvent-free procedure) under elevated temperatures (i.e., to graft dPG from the MI-dPG coating) (Figure 1). By following this strategy, the direct grafting of antifouling dPG from the surface was extended to a wide variety of substrates, resulting from the substrate-independent adhesion character of the MI-dPG coating. In the presented work, hydrophilic titanium dioxide and hydrophobic PDMS were used as substrate materials. These materials were selected because of their relevance in biomedical applications. Furthermore, these materials showed large variations in their chemical and physical surface properties. Therefore, the functionalization of these materials provided a proof-of-concept for the substrate-independent applicability of the novel method presented in this
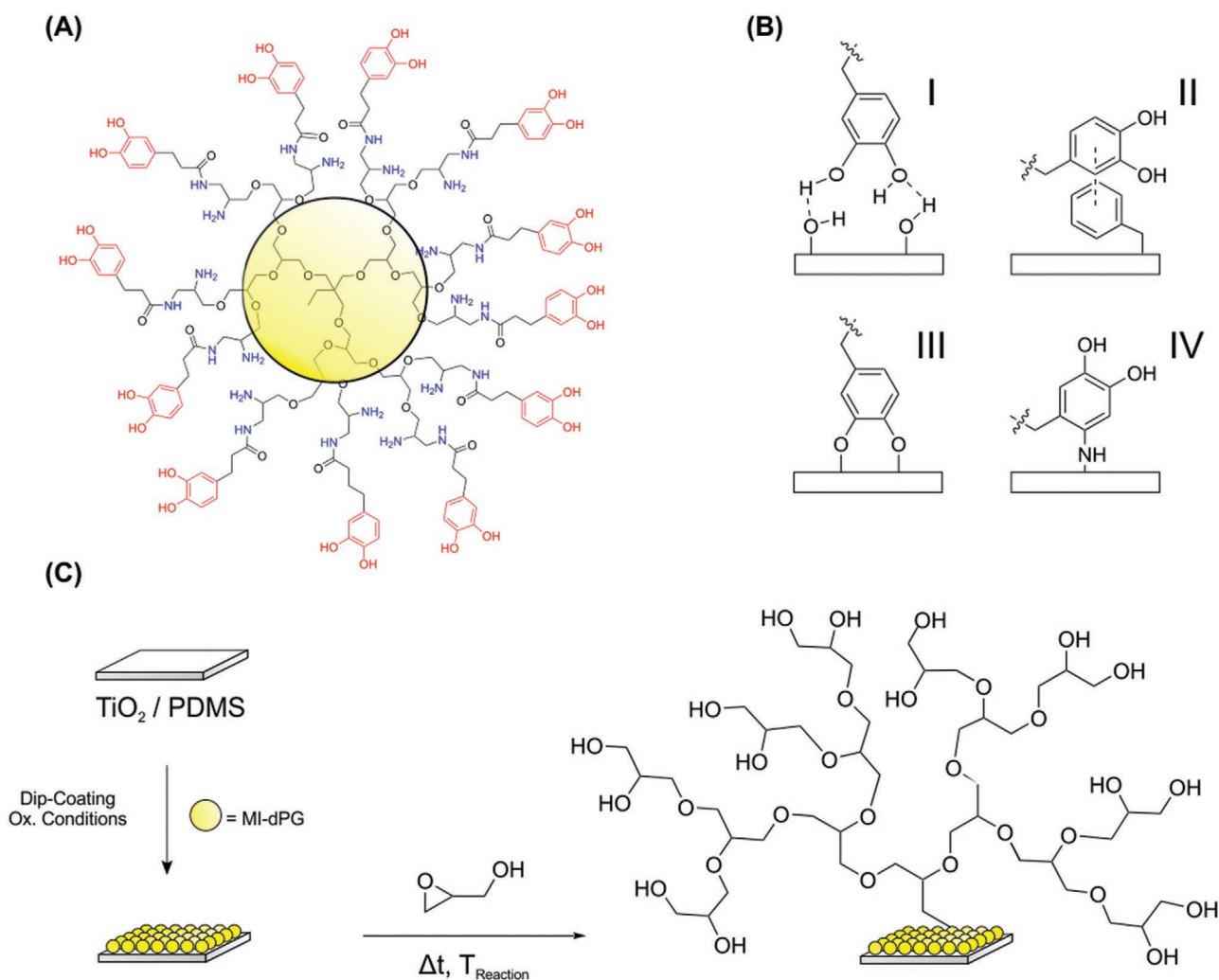
Figure 1. A) A schematic representation of the molecular structure of MI-dPG. The shown structure is an idealized molecular structure; the number of glycerol monomer (shown within the yellow sphere) varies with the size of the polymer. The dPG-core shows ≈55% branching.[31] The catechol moieties are depicted in red. The amine moieties are depicted in blue. B) The various ways in which catechols can adhere to the surface. I) On surfaces that contain hydrogen bond donors/acceptors, catechols can adhere via hydrogen bond formation, II) on surfaces that contain aromatic systems, catechols can bind via π–π interactions, III) catechols can tether to certain metal oxide surfaces (especially TiO_2) via the formation of strong but reversible metal complexes, IV) finally, catechols can irreversibly bind to amine (and thiol) functionalized surfaces via the formation of Michael adducts and Schiff bases.[14] C) A schematic representation of the surface functionalization steps that were performed in this work. After the coating of TiO_2 and PDMS with MI-dPG, the MI-dPG coating was utilized as a macro-initiator for the thermally induced ring-opening polymerization of glycidol from the surface (i.e., the grafting of dPG). The polymerization of dPG from the surface could be initiated through the amine and catechol functional groups of the MI-dPG coating.

work. It was hypothesized that the thickness and morphology of the grafted dPG-layer would vary as a function of the reaction time and temperature. Furthermore, an earlier work by our group showed that the covalent immobilization of dPG on MI-dPG coatings (i.e., utilizing a "grafting to" approach) leads to the formation of surfaces that effectively prevent the adhesion of bovine serum albumin and fibrinogen.[30] Therefore, it was expected that the introduction of a dPG-layer via the direct grafting of glycidol from the MI-dPG coating would also lead to the formation of potent antifouling surfaces.[28,29]

2. Results and Discussion

First, transparent TiO_2-coated substrates were produced according to Section S1.2.1 in the Supporting Information (i.e.,

a transparent model coating with the surface properties of bulk titanium). Subsequently, these substrates were functionalized with MI-dPG, according to a modified version of the dip coating method that was earlier described by Wei et al. (Sections S1.1.4. and S1.2.3. in the Supporting Information).[19] After dip coating, the MI-dPG-coated surfaces were put in a substrate holder in a custom made flask at 110 °C under high vacuum for >10 h (from now on referred to as TiO₂–MI-dPG$_{110 °C, HV}$) (Figure S1, Supporting Information), ensuring that all solvent was removed from the coatings prior to the grafting process. Interestingly, this drying process led to an increase in the CA, when the coatings were compared to MI-dPG coatings that were dried under atmospheric pressure for one hour at 50 °C (from now on referred to as TiO₂–MI-dPG$_{50 °C, ATM}$) (Figure S3 and Table S1, Supporting Information). This observation was explained by further intralayer crosslinking of the MI-dPG coating under

2000931 (3 of 11)

ADVANCED
SCIENCE NEWS
www.advancedsciencenews.com

ADVANCED
MATERIALS
INTERFACES
www.advmatinterfaces.de

elevated temperatures and high vacuum, effectively leading to a loss of free amines, therefore effectively making the coating less hydrophilic. Analysis of TiO$_2$–MI-dPG$_{50\,°C,\,ATM}$ by X-ray photoelectron spectroscopy (XPS) showed a 1.35:1 ratio of C—O to C—C bonds (Figure 3A; Tables S3 and S4, Supporting Information), which was roughly in line with an earlier work of our group.[20a] For TiO$_2$–MI-dPG$_{110\,°C,\,HV}$ the C—O bond content of the MI-dPG coating slightly decreased to a 1.09:1 ratio of C—O to C—C bonds. Additionally, the N1s' elemental content observed for TiO$_2$–MI-dPG$_{50\,°C,\,ATM}$ was clearly higher than the N1s' elemental content observed for TiO$_2$–MI-dPG$_{110\,°C,\,HV}$ (Figure 3C; Figure S5 and Table S5, Supporting Information). These observations were explained by the occurrence of additional Michael-type addition reactions and the formation of Schiff bases between the *o*-quinones and free amines present in the MI-dPG coating under vacuum at elevated temperatures. A slightly higher Ti2p content was observed for TiO$_2$–MI-dPG$_{110\,°C,\,HV}$ than for TiO$_2$–MI-dPG$_{50\,°C,\,ATM}$, indicating that the coating decreased its thickness as a result of the drying process at elevated temperatures under reduced pressure (Figure 3C; Figure S5 and Table S5, Supporting Information). The combined results suggested the additional crosslinking and shrinkage of the coating upon heating at elevated temperatures under vacuum conditions. This additional crosslinking might have positively contributed to the stability of the MI-dPG coating on the surface. The drying process was required in order to covalently graft dPG from the MI-dPG coating, as remaining solvent could potentially quench the dPG grafting reaction. Therefore, all coatings that are further discussed in the current work were polymerized from MI-dPG coatings that were previously dried at 110 °C under high vacuum, unless stated otherwise. The data for TiO$_2$–MI-dPG$_{50\,°C,\,ATM}$ were only included to indicate that further crosslinking of the MI-dPG coating occurs upon the drying of the coating under high vacuum at elevated temperatures.

To determine the optimal dPG grafting time and temperature (i.e., the time and temperature that would result in the lowest CA), glycidol was grafted from TiO$_2$–MI-dPG for t = 30 min, 1, 3, and 24 h at 80, 100, and 120 °C (from now on referred to as TiO$_2$–MI-dPG@dPG$_{\Delta t,\,T}$, with Δt = reaction time and T = reaction temperature) (Section S1.2.4. in the Supporting Information). A time- and temperature-dependent decrease of the CA was clearly observed after the grafting of dPG from the MI-dPG-coated substrates (**Figure 2**A,B; Figure S4 and Table S2, Supporting Information). CA measurements showed surface wetting for TiO$_2$–MI-dPG@dPG$_{3h,\,100\,°C}$ and TiO$_2$–MI-dPG@dPG$_{24h,\,80\,°C}$ (Figure 2A,B; Figure S4 and Table S2, Supporting Information). Interestingly, when the grafting process was performed at 120 °C the CA reached ≈25°, i.e., no surface wetting was observed. This observation was explained by a synergetic effect between the surface roughness and the hydrophilic surface chemistry in case of TiO$_2$–MI-dPG@dPG$_{3h,\,100\,°C}$ and TiO$_2$–MI-dPG@dPG$_{24h,\,80\,°C}$, significantly lowering the CA obtained for these substrates. When the grafting process was performed at higher reaction temperatures or with longer reaction times, the (nanometer-sized) surface roughness was potentially lost as a result of excessive dPG grafting. Consequently, CA values that are common for polyglycerol monolayer coatings were observed in case of longer grafting times with high reaction
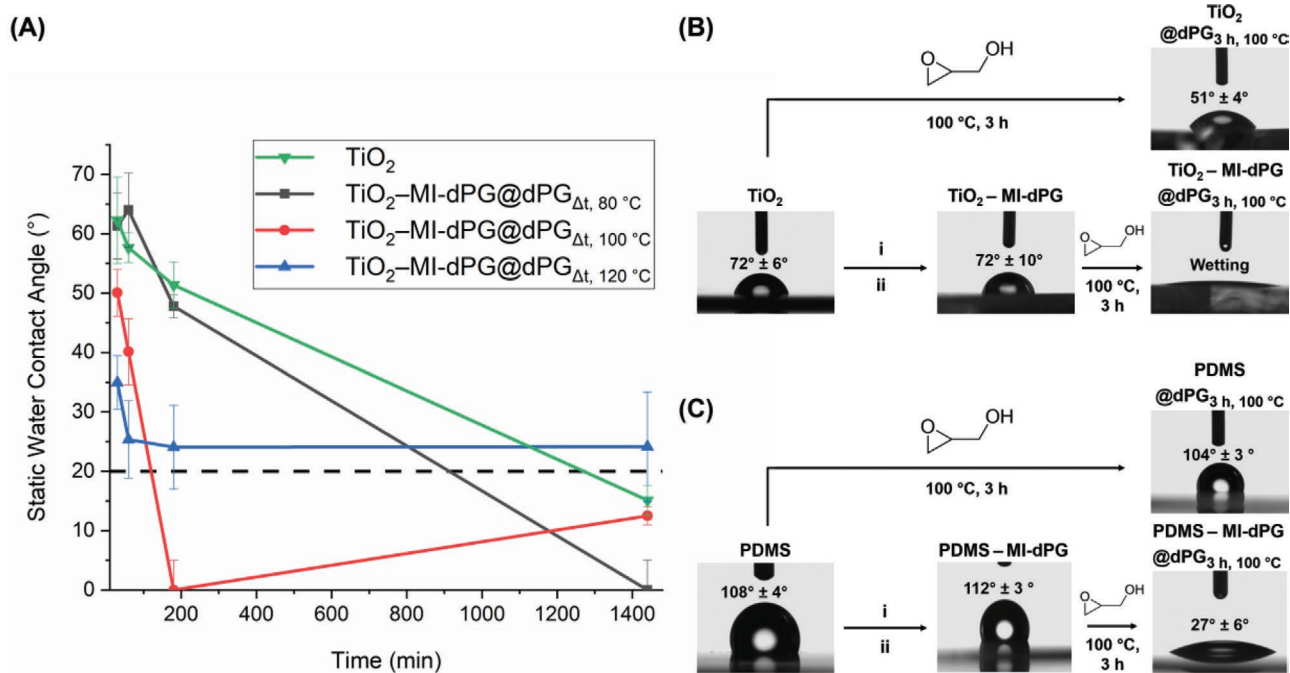

Figure 2. A) A graphical representation of the CA obtained for TiO$_2$ (green), TiO$_2$–MI-dPG@dPG$_{\Delta t,\,80\,°C}$ (black), TiO$_2$–MI-dPG@dPG$_{\Delta t,\,100\,°C}$ (red), and TiO$_2$–MI-dPG@dPG$_{\Delta t,\,120\,°C}$ (blue) as a function of the time (in minutes). The dotted black line represents the CA obtained for a polyglycerol monolayer on gold.[26] All measurements were performed as triplicates; the error bars represent the standard deviation from the mean. B) The CA images obtained for TiO$_2$, TiO$_2$@dPG$_{3h,\,100\,°C}$, TiO$_2$–MI-dPG, and TiO$_2$–MI-dPG@dPG$_{3h,\,100\,°C}$. The shown CA values were obtained from measurements that were performed in triplicate. The shown error reflects the standard deviation from the mean. i): coating with MI-dPG, ii): drying under high vacuum at 110 °C.

**ADVANCED
SCIENCE NEWS**

www.advancedsciencenews.com

**ADVANCED
MATERIALS
INTERFACES**

www.advmatinterfaces.de

temperatures.[26] The combined results showed the successful grafting of dPG from the MI-dPG coated TiO$_2$ substrate.

As a control, bare TiO$_2$ substrates were incubated with glycidol for t = 30 min, 1, 3, and 24 h at 100 °C (from now on referred to as TiO$_2$@dPG$_{\Delta t, 100 °C}$) (Section S1.2.4, Supporting Information). CA measurements of TiO$_2$@dPG$_{\Delta t, 100 °C}$ showed a time-dependent decrease in the CA, which was explained by the grafting of dPG from hydroxyl moieties present on the TiO$_2$ substrates (Figure 2A,B; Figure S4 and Table S2, Supporting Information). The results observed for the bare TiO$_2$ were in line with an earlier work by Weber et al.[29] Nevertheless, surface wetting was not observed for TiO$_2$@dPG$_{\Delta t, 100 °C}$. Furthermore, the CA value obtained for TiO$_2$@dPG$_{3h, 100 °C}$ clearly exceeded the CA-value obtained for TiO$_2$–MI-dPG@dPG$_{3h, 100 °C}$ (51° ± 4° and surface wetting, respectively), indicating that the grafting process was insufficient in absence of the MI-dPG coating (Figure 2A,B; Figure S4 and Table S2, Supporting Information).

When the grafting process was characterized by means of XPS, a time-dependent increase of the C—O bond content was observed for TiO$_2$–MI-dPG@dPG$_{\Delta t, T}$ with T = 80, 100, or 120 °C and TiO$_2$@dPG$_{\Delta t, 100 °C}$. However, for TiO$_2$@dPG$_{\Delta t, 100 °C}$ the C—O bond content increased only slowly, whereas high C—O contents were already observed after 30 min of dPG grafting for all MI-dPG-coated systems at all tested temperatures (**Figure 3**B; Tables S6 and S7, Supporting Information). These observations further confirmed that the MI-dPG coating accelerated the dPG grafting process. Additionally, for TiO$_2$–MI-dPG@dPG$_{\Delta t, T}$, it was observed that the C—O content (and thus the dPG-layer) increased quicker when the dPG grafting was performed at higher temperatures (Figure 3B; Tables S6 and S7, Supporting Information). When the elemental contents of titanium (i.e., the Ti2p elemental content) and nitrogen (i.e., the N1s elemental content) were investigated by means of XPS, a time-dependent decrease in the Ti2p content was observed for TiO$_2$@dPG$_{\Delta t, 100 °C}$, which indicated the successful but slow grafting of dPG from the surface (Figure S5 and Table S8, Supporting Information); Only after 24 h of dPG grafting the Ti2p elemental content was clearly reduced on the bare TiO$_2$-substrate (Figure S5 and Table S8, Supporting Information). When the elemental compositions of TiO$_2$–MI-dPG@dPG$_{\Delta t, T}$ were assessed by means of XPS, low but measurable Ti2p elemental contents were observed for TiO$_2$–MI-dPG and for TiO$_2$–MI-dPG@dPG$_{\Delta t, 80 °C}$ with Δt = 30 min, 1, or 3 h (Figure S5 and Table S8, Supporting Information). Only after 24 h of dPG grafting no Ti2p content was observed for TiO$_2$–MI-dPG@dPG$_{24h, 80 °C}$. In case of TiO$_2$–MI-dPG@dPG$_{\Delta t, T}$ with T = 100 or 120 °C, the Ti2p signal was already non-observable after 1 h of dPG grafting, indicating that the dPG-layer was already thick enough (i.e., >10 nm) to completely suppress the Ti2p signal (Figure 3C; Figure S5 and Table S8, Supporting Information), i.e., showing that the grafting process occurred quicker at higher temperatures.

The speed of the dPG grafting process from the MI-dPG-coated TiO$_2$ substrates could also be followed by monitoring the N1s elemental content (the N1s signal originated from the amines present in the MI-dPG coating): a time-dependent decrease of the N1s content was clearly observed as a function of the reaction time, which indicated the grafting of the dPG-layer from the MI-dPG coating (Figure 3C; Figure S5

and Table S8, Supporting Information). Furthermore, it was observed that at higher temperatures the N1s signal decreased faster than at lower temperatures, which showed that the dPG grafting process occurred the fastest at 120 °C (Figure S5; Table S8, Supporting Information) and the slowest at 80 °C.

Many works have shown the relation between surface wettability and antifouling surface properties (i.e., protein and cell-repelling properties) for hydrophilic non-charged polymeric coatings.[5] In the present work, the combined results showed the successful grafting of hydrophilic antifouling dPG from MI-dPG-coated TiO$_2$ at all tested temperatures, and the lowest CA values were obtained for TiO$_2$–MI-dPG@dPG$_{3h, 100 °C}$ and TiO$_2$–MI-dPG@dPG$_{24h, 80 °C}$. The grafting of dPG at <80 °C would result in extended reaction times (>24 h) in order to observe surface wetting, making the process less interesting from an industrial point of view, whereas dPG grafting at >120 °C would most likely not lead to the observation of surface wetting, resulting from rapid and excessive dPG grafting.

To show the wider applicability of the developed dPG grafting process, hydrophobic polydimethylsiloxane (PDMS) was coated with MI-dPG (from now on referred to as PDMS–MI-dPG) and subsequently incubated with glycidol (Sections S1.2.2–S1.2.4 in the Supporting Information). It is important to notice, that in case of PDMS the catechols were more likely to mediate surface binding via the formation of hydrogen bonds (i.e., analogous to the binding of catechols to hydroxylated silica surfaces) (Figure 1B), rather than via the formation of strong reversible coordination complex structures (such as in case of catechol-binding to TiO$_2$ substrates).[14] Therefore, the dPG grafting procedure was repeated with PDMS, in order to ensure the stability of the MI-dPG coating under the reaction conditions that were required for the grafting of dPG from the MI-dPG coating. As industrial applications favor solvent-free reactions with short reactions times (i.e., enhancing productivity while lowering production costs), PDMS–MI-dPG was only incubated with glycidol under the optimized reaction conditions which were obtained from the dPG grafting from TiO$_2$–MI-dPG (i.e., 3 h at 100 °C). As a control, bare PDMS was incubated with glycidol under identical conditions. Analysis of PDMS@dPG$_{3h, 100 °C}$ by means of CA measurements showed no significant change in the wetting characteristics of the PDMS surface after the dPG grafting process, which indicated that dPG was insufficiently grafted from the bare PDMS surface (Figure 2C). The CA obtained for the PDMS–MI-dPG surface showed a slightly decreased wetting character in comparison to the bare PDMS substrate, which was explained by the combination of the intrinsic hydrophobic character of PDMS (initial CA: 108° ± 4°) and the roughness introduced to the PDMS surface by the MI-dPG coating (Figure 2C). When PDMS–MI-dPG was subsequently incubated with glycidol, a clear decrease in the CA was observed (CA for PDMS–MI-dPG@dPG$_{3h, 100 °C}$: 27° ± 6°), which was explained by the successful grafting of dPG from the MI-dPG coating (Figure 2C). Analysis of the bare PDMS substrate by means of XPS showed the high prevalence of a Si—C bond content and the absence of C—O bonds (Figure 3D; Tables S9 and S10, Supporting Information).[32] When PDMS was incubated with glycidol at 100 °C for 3 h, only a slight increase in the C—O content was observed, which further indicated the insufficient grafting of dPG from the bare PDMS
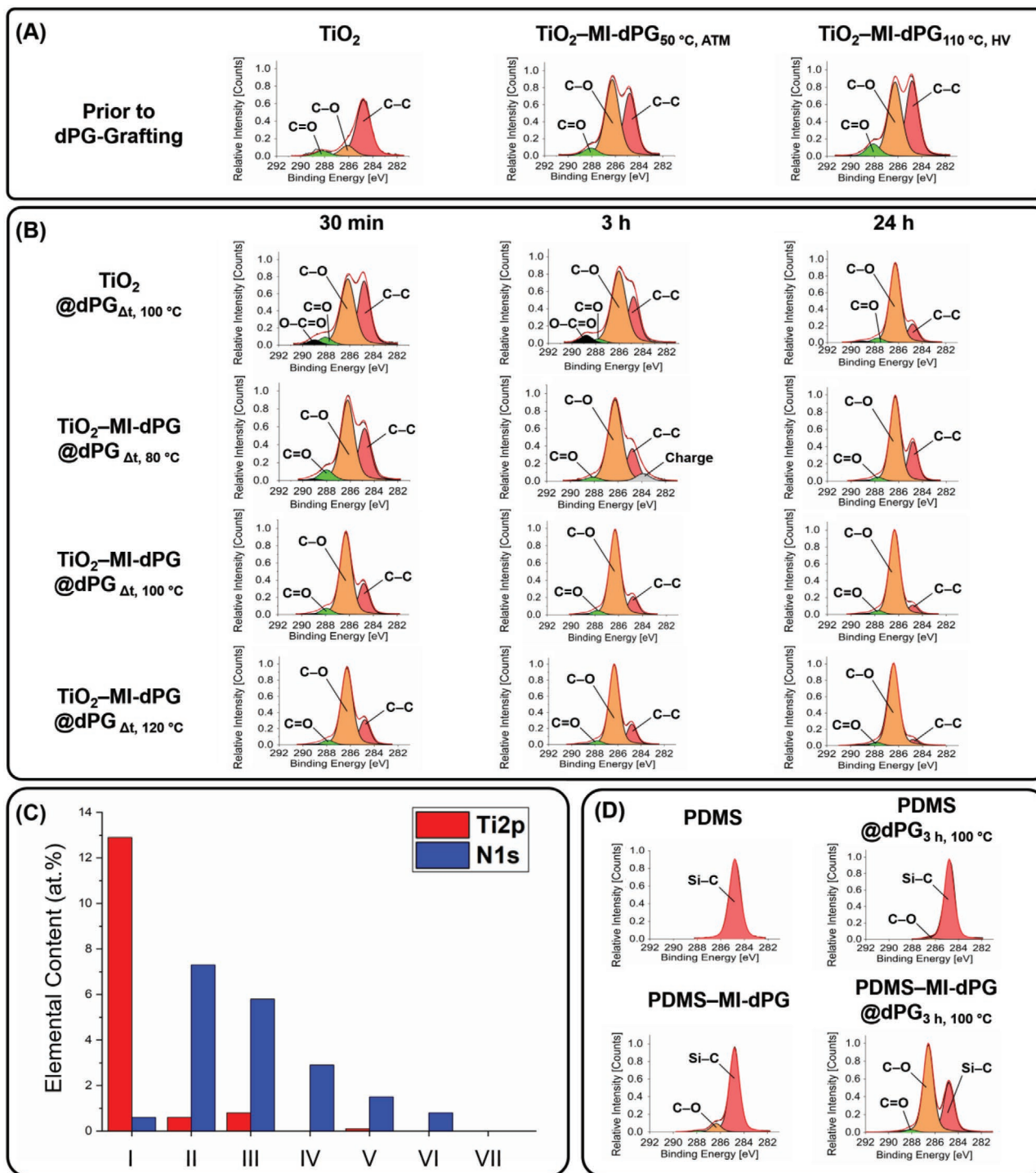
Figure 3. A) Highly resolved C1s spectra of TiO_2, TiO_2–MI-dPG$_{50\,°C,\,ATM}$, and TiO_2–MI-dPG$_{110\,°C,\,HV}$. B) Highly resolved C1s spectra of TiO_2@dPG$_{\Delta t,\,100\,°C}$, TiO_2–MI-dPG@dPG$_{\Delta t,\,80\,°C}$, TiO_2–MI-dPG@dPG$_{\Delta t,\,100\,°C}$, and TiO_2–MI-dPG@dPG$_{\Delta t,\,120\,°C}$. C) The Ti2p (red) and N1s (blue) content of I) the bare TiO_2-substrate, II) TiO_2–MI-dPG$_{50\,°C,\,ATM}$, III) TiO_2–MI-dPG$_{110\,°C,\,HV}$, IV) TiO_2–MI-dPG@dPG$_{30\,min,\,100\,°C}$, V) TiO_2–MI-dPG@dPG$_{1h,\,100\,°C}$, VI) TiO_2–MI-dPG@dPG$_{3h,\,100\,°C}$, VII) TiO_2–MI-dPG@dPG$_{24h,\,100\,°C}$. D) The XPS spectra obtained for PDMS, PDMS@dPG$_{3h,\,100\,°C}$, PDMS–MI-dPG, and PDMS–MI-dPG@dPG$_{3h,\,100\,°C}$.

substrate (Figure 3D; Tables S9 and S10, Supporting Information). When PDMS–MI-dPG was assessed by means of XPS, the highly resolved C1s spectrum showed the slight presence of C–O content (Figure 3D; and Tables S9 and S10, Supporting

Information), which was explained by the formation of the MI-dPG coating on PDMS. Analysis of PDMS–MI-dPG@dPG$_{3h,\,100\,°C}$ showed a clear increase in the C–O content in respect to the PDMS–MI-dPG substrate (Figure 3D; Tables S9
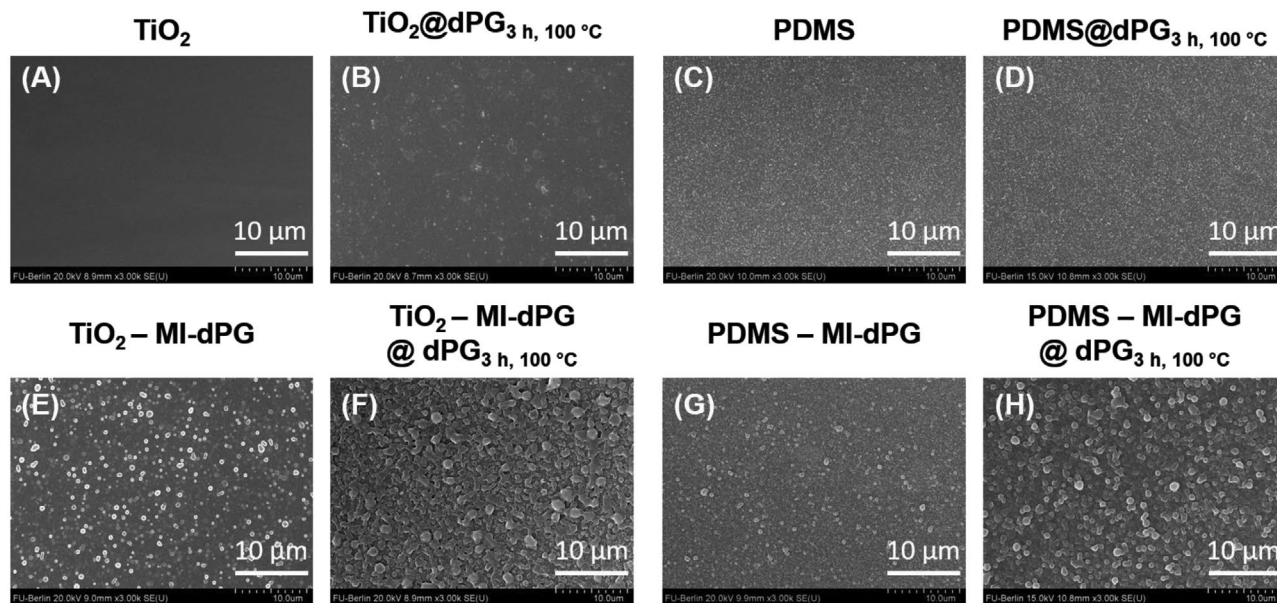
ADVANCED
Science News
www.advancedsciencenews.com

ADVANCED
MATERIALS
INTERFACES
www.advmatinterfaces.de

Figure 4. SEM images of the A) bare TiO$_2$-substrate, B) the TiO$_2$@dPG$_{3h, 100 °C}$, C) PDMS, D) PDMS@dPG$_{3h, 100 °C}$, E) TiO$_2$–MI-dPG, F) TiO$_2$–MI-dPG@dPG$_{3h, 100 °C}$, G) PDMS–MI-dPG, and H) PDMS–MI-dPG@dPG$_{3h, 100 °C}$. The shown images are a 3000× enlargement of the measured surface.

and S10, Supporting Information), indicating the successful grafting of dPG from the MI-dPG coating on PDMS. When the elemental contents of silicon (i.e., the Si2p elemental content) and nitrogen (i.e., the N1s elemental content) were assessed for the various PDMS-based systems by means of XPS, a high Si2p signal was observed for the bare PDMS substrate (Figure S6 and Table S11, Supporting Information). After incubation with glycidol at 100 °C for 3 h, the Si2p signal did only show a minor change, which indicated that dPG was insufficiently grafted from the bare PDMS substrate (Figure S6 and Table S11, Supporting Information). Analysis of the elemental content of the PDMS–MI-dPG substrate showed a clear reduction in the Si2p content in respect to the bare PDMS substrate (Figure S6 and Table S11, Supporting Information). Additionally, a higher N1s content was observed for PDMS–MI-dPG than for the bare PDMS substrate (Figure S6 and Table S11, Supporting Information). The combined results indicated the successful formation of the MI-dPG coating on PDMS. The grafting of dPG from the PDMS–MI-dPG substrate led to a clear decrease in the observed Si2p content, indicating the successful formation of the dPG layer on top of the MI-dPG layer (Figure S6 and Table S11, Supporting Information). Additionally, the N1s content for PDMS–MI-dPG@dPG$_{3h, 100 °C}$ was lower than for PDMS–MI-dPG, further confirming the successful grafting of dPG from the MI-dPG coating (Figure S6 and Table S11, Supporting Information).

When the surface morphology of the dPG grafting process was investigated by means of scattering electron microscopy (SEM), it was clearly observed that the MI-dPG coating introduced roughness in the micrometer range to the bare TiO$_2$ and PDMS substrates (**Figure 4**A,C,E,G). This observation was in line with earlier works of our group.[19,20,33] When the MI-dPG-coated substrates were subsequently incubated with glycidol at 100 °C for 3 h, a further increase in the surface roughness was clearly observed (Figure 4F,H). In the case

of TiO$_2$–MI-dPG@dPG$_{3h, 100 °C}$, the grafted dPG appeared as merging smeared out micrometer-sized particles. For PDMS–MI-dPG@dPG$_{3h, 100 °C}$, the grafted particles appeared less smeared out, indicating that the dPG grafting process from PDMS–MI-dPG might have occurred slower than from the TiO$_2$–MI-dPG substrate. Nevertheless, in both cases the SEM images clearly showed the successful grafting of dPG from the MI-dPG adhesive layer. When the bare TiO$_2$ substrate was incubated with glycidol at 100 °C for 3 h, some particles were observed on the surface (Figure 4B). However, the obtained SEM images clearly showed the enhanced grafting of dPG in the presence of the MI-dPG coating. When bare PDMS was incubated with glycidol under elevated temperatures, no clear changes in the surface morphology were observed (Figure 4D). For additional images of the dPG grafting process from TiO$_2$, TiO$_2$–MI-dPG, PDMS, and PDMS–MI-dPG (showing additional grafting times and temperatures), the reader is referred to Figures S7 and S8 in the Supporting Information.

The viability of adhesive human adenocarcinoma cells (A549 cells) and chicken fibroblast cells (DF-1 cells) was investigated on the various substrates by means of LIVE/DEAD staining (Sections S1.3.1. and S1.3.2., Supporting Information). High cells numbers were observed for both the A549 and DF-1 cells on tissue culture polystyrene (TCPS) control. However, the A549 cells showed higher adhesion than the DF-1 cells under the set incubation conditions (**Figures 5**A, **6**A,B; Table S12, Supporting Information), even when the DF-1 cells were seeded at a 5 times higher concentration than the A549 cells. This observation was explained by different proliferation rates of the two cell types on the TCPS substrate (the shown images were taken after 24 h of culturing) (Figures 5A, 6C,D; and Table S12, Supporting Information). Additionally, both cell types showed high viability on TCPS. High cell numbers with high cell viabilities were also observed for both the A549 and DF-1 cells on the bare TiO$_2$ and PDMS substrates (Figures 5B,C, 6A–D; Table S12,
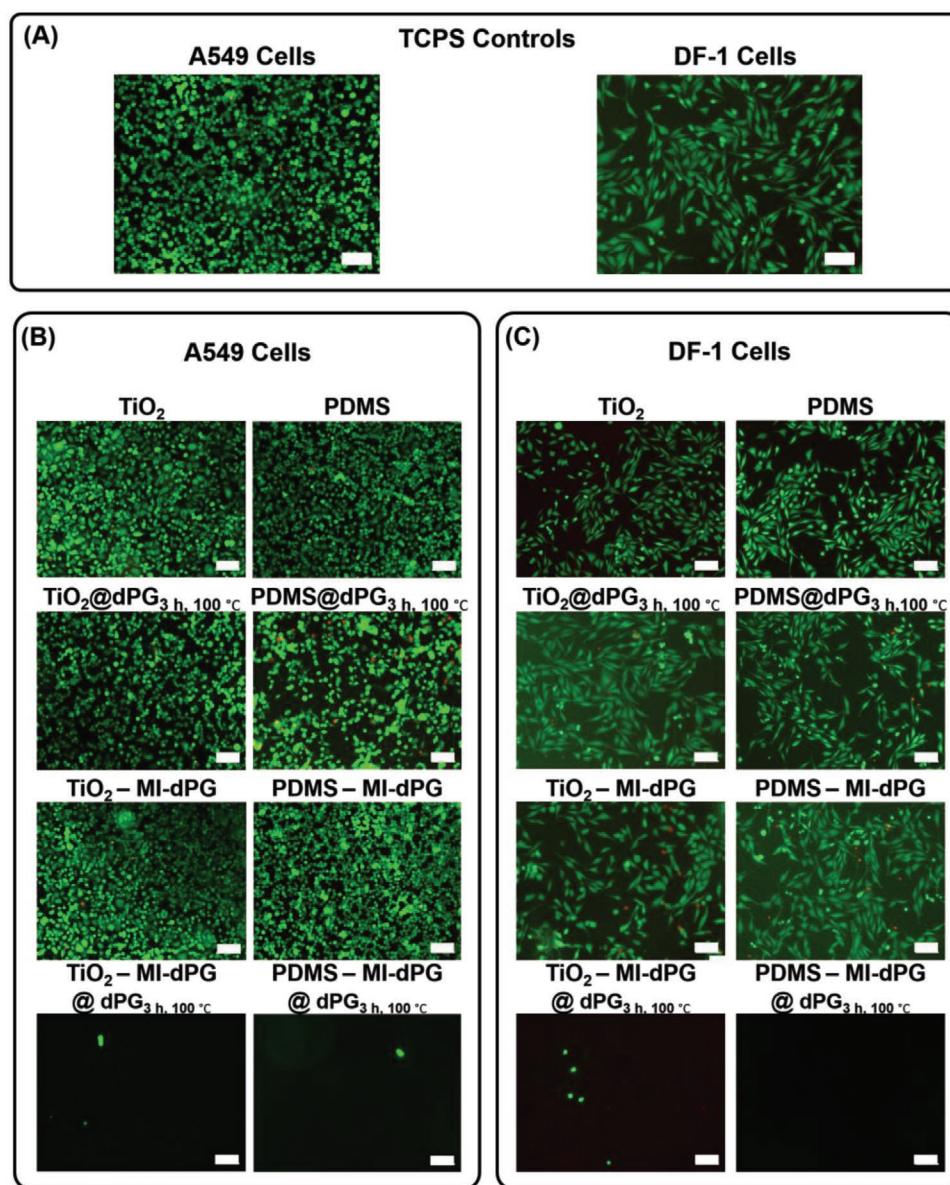
Figure 5. The images obtained after LIVE/DEAD staining A) live cells appear in green, whereas dead cells appear in red. The white bar represents 100 µm. B) The images obtained for the A549 cells on the various coating types. C) The images obtained for the DF-1 cells for the various coating conditions.

Supporting Information). As a control, the proliferation of A549 and DF-1 cells was also investigated on $TiO_2@dPG_{3h, 100 °C}$ and $PDMS@dPG_{3h, 100 °C}$ (Figures 5B,C, 6A–D; Table S12, Supporting Information). No significant changes in the cell numbers were observed for $TiO_2@dPG_{3h, 100 °C}$ for both cell types, when the substrate was compared to bare TiO_2 (Figures 5B and 6A; Table S12, Supporting Information), and for $PDMS@dPG_{3h, 100 °C}$ similar results were obtained (Figures 5B and 6A; Table S12, Supporting Information). The cells observed on $TiO_2@dPG_{3h, 100 °C}$ and $PDMS@dPG_{3h, 100 °C}$ showed high viability (Figures 5B,C, 6C,D; Table S12, Supporting Information). The results were explained by the insufficient grafting of the dPG-layer from the TiO_2 or PDMS substrates after 3 h of dPG grafting at 100 °C (as earlier confirmed by CA measurements,

XPS, and SEM), i.e., in the absence of a sufficient dPG layer no antifouling properties were to be expected. On TiO_2–MI-dPG, no significant change in the A549 cell number was observed, when the substrate was compared to the bare TiO_2 substrate (Figures 5B and 6A; Table S12, Supporting Information of the ESI). However, the number of DF-1 cells on TiO_2–MI-dPG was found to be significantly lower than for the bare TiO_2 substrate (Figures 5C and 6B; Table S12, Supporting Information). For the PDMS–MI-dPG substrate, similar results were obtained (Figures 5C and 6B; Table S12, Supporting Information). Besides, the cell viabilities of both cell types were found to be high on the TiO_2–MI-dPG and PDMS–MI-dPG substrates (Figures 5B,C, 6C,D; Table S12, Supporting Information). The variations observed in the cell proliferation on the

ADVANCED
SCIENCE NEWS

www.advancedsciencenews.com

ADVANCED
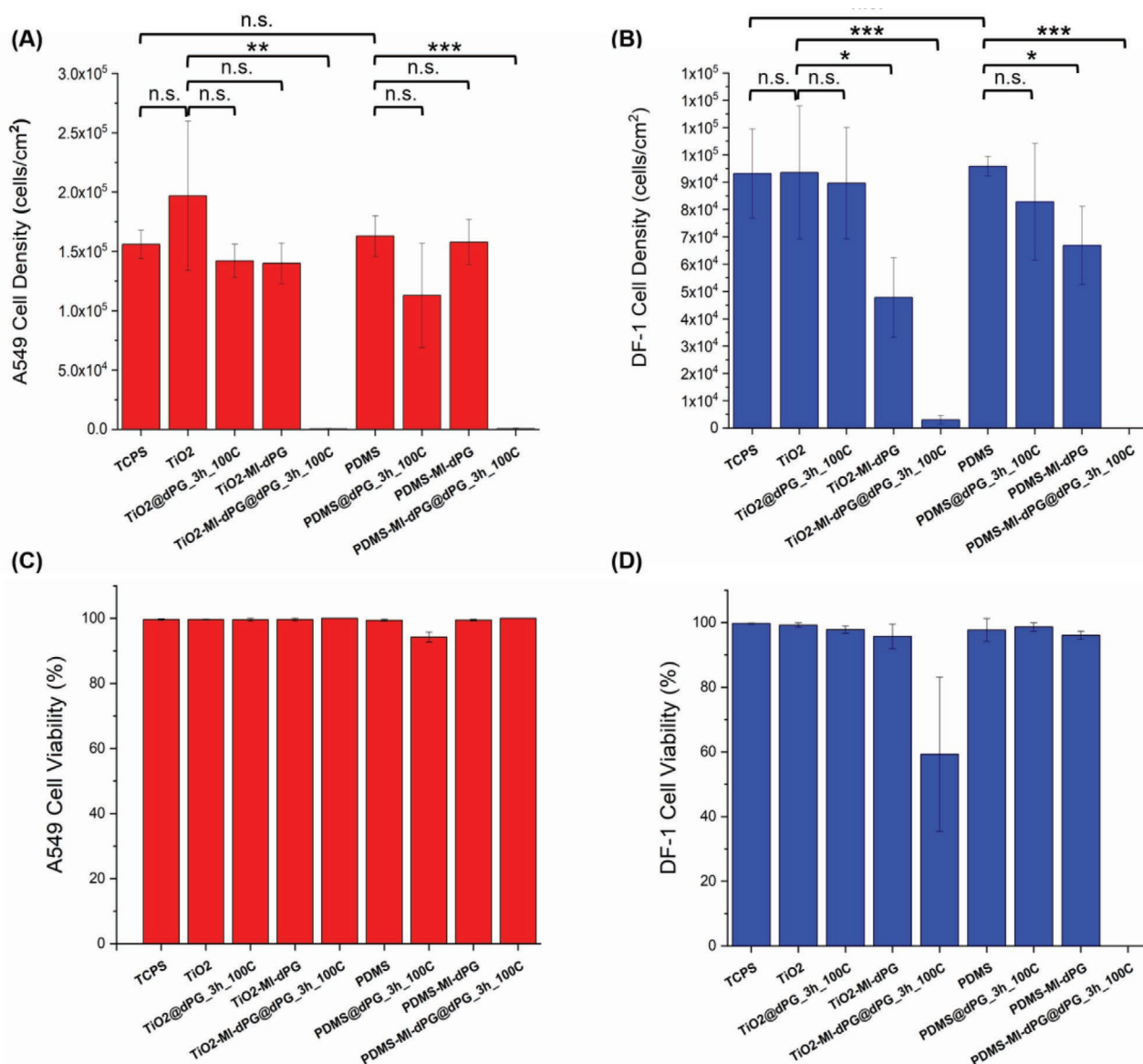**MATERIALS**
INTERFACES

www.advmatinterfaces.de

Figure 6. A) A graph showing the A549 cell density on the various substrates. B) A graph showing the DF-1 cell density on the various substrates. C) The cell viability of the A549 cells on the various substrates as obtained via LIVE/DEAD cell staining. D) The cell viability of the DF-1 cells on the various substrates as obtained via LIVE/DEAD cell staining. The viability for the DF-1 cells on $TiO_2–MI\text{-}dPG@dPG_{3h, 100\,°C}$ was calculated from a low amount of cells, therefore the presence of only a few dead cells heavily influenced the observed viability (Table S12, Supporting Information). The viability of the DF-1 cells on $PDMS–MI\text{-}dPG@dPG_{3h, 100\,°C}$ could not be determined as a result of the total absence of cells (Table S12, Supporting Information). The shown error bars show the standard deviation from the mean. The cell numbers were quantified using at a minimum of three images per substrate type. $*p = 0.05$; $**p = 0.01$; $***p = 0.001$. The p values were calculated utilizing a two-tailed t-test under the assumption of equal variance.

MI-dPG coatings were in line with the results of Lee et al., who showed that PDA films can either be cytophilic or cytophobic depending on the cell line.[16] Further functionalization of the MI-dPG coating with growth factors might be necessary in order to promote the proliferation of certain cell types (e.g., for DF-1 cells).[34] Quantification of the A549 and DF-1 cells showed a dramatic decrease in the cell numbers of both cell types after the grafting of dPG from TiO₂–MI-dPG and PDMS–MI-dPG. In case of $TiO_2–MI\text{-}dPG@dPG_{3h, 100\,°C}$, a $> 95\%$ reduction of the cell density was observed for both cell types, when compared

to the bare TiO₂ substrate (Figures 5B, 6A,B; Table S12, Supporting Information). Similar results were obtained for PDMS–$MI\text{-}dPG@dPG_{3h, 100\,°C}$ (Figures 5C, 6A,B; Table S12, Supporting Information). When the viability of the A549 cells on the TiO_2–$MI\text{-}dPG@dPG_{3h, 100\,°C}$ and PDMS–$MI\text{-}dPG@dPG_{3h, 100\,°C}$ substrates was studied, it was observed that the majority of the cells appeared alive, indicating the high biocompatibility of both surfaces (Figures 5B,C, 6C,D; Table S12, Supporting Information). When the viability of the DF-1 cells was studied on TiO₂–$MI\text{-}dPG@dPG_{3h, 100\,°C}$, lower cell viability was observed

resulting from a general low amount of cells present on the surface, i.e., only a few dead cells greatly influenced the viability in this case. In case of the PDMS–MI-dPG@dPG$_{3h, 100\,°C}$ no adherent cells were observed, and therefore it was not possible to calculate the viability on this substrate. An earlier work by our group utilized dPG for the introduction of antifouling surface properties and additionally showed the general biocompatibility and non-toxicity of dPG.[30] Therefore, it is to be expected that both TiO$_2$–MI-dPG@dPG$_{3h, 100\,°C}$ and PDMS–MI-dPG@dPG$_{3h, 100\,°C}$ will be non-toxic toward a broad spectrum of cell types, while being highly cell-repelling. The dramatic reduction in the cell numbers of both cell types after the grafting of dPG from the MI-dPG-coated substrates was explained by the effective formation of a surface hydration layer, which formed a physical barrier that prevented cell adhesion.[5]

3. Conclusions

In the current work, a novel universal method for the grafting of dPG from mussel-inspired adhesion layers was achieved. The successful grafting of dPG from TiO$_2$–MI-dPG and PDMS–MI-dPG was confirmed by means of CA measurements, XPS, and SEM. Additionally, it was shown that the dPG grafting process occurred insufficiently in the absence of the MI-dPG coating on both substrate types.

When the viability of A549 and DF-1 cells on the various coatings was investigated, high numbers of viable cells were observed on the tissue culture polystyrene control, on the bare TiO$_2$, and on the PDMS substrate. Introduction of the MI-dPG coating to the TiO$_2$ and PDMS substrates did not influence the A549 cell numbers, whereas the DF-1 cell numbers slightly decreased. Subsequent dPG grafting from the MI-dPG coatings led to a dramatic decrease (>95%) in the cell numbers of both cell types for both substrate types. The reduced cell numbers were explained by the successful formation of a surface hydration layer on the dPG-grafted coating, which prevented the adhesion of cells. The combined results showed that the grafting of dPG from MI-dPG-coated substrates provides a successful strategy for the creation of cell-repelling but highly biocompatible surfaces.

The method developed in the current work gives exact control over the wettability of the substrate (i.e., CA values from 60° till <10° were easily achieved by adjusting the reaction time and temperature) while maintaining the chemical characteristics of the surface (i.e., effectively a dPG surface with tunable CA was developed). Resulting from the substrate-independent adhesion character of the MI-dPG polymer,[19] the method presented in the current work could be utilized to graft dPG from a broad spectrum of substrates, independent from the chemical or physical characteristics of the substrate materials. Therefore, the direct grafting of antifouling dPG as developed in earlier works,[28,29] can now be extended to a broad range of (medically relevant) hydrophilic and hydrophobic substrates (e.g., prosthetic materials, cardiovascular implant materials, and materials for implantable biosensors). Additionally, the dPG grafting process was performed in bulk (i.e., solvent-free), in the absence of caustic bases, and without activation of the substrate material prior to the grafting process, following a simple two-step procedure (i.e., first MI-dPG coating of the substrate and then the grafting of dPG from the MI-dPG coating).

Future works could utilize atomic force microscopy (AFM) to precisely investigate the relation between the surface (nanoscale) roughness and the antifouling surface properties of dPG-grafted MI-dPG coatings, i.e., AFM could be utilized to further optimize the antifouling performance of dPG-grafted MI-dPG coatings. Additionally, future works could focus on the grafting of alternative commercially available glycidyl ethers such as glycidyl 2,2,3,3,4,4,5,5-octafluoropentyl ether and dodecyl glycidyl ethers from the MI-dPG coating, e.g., for the creation of mussel-inspired (super)hydrophobic surfaces.

4. Experimental Section

All materials and (analytical) methods are described in Sections S1.1–S1.3 in the Supporting Information.

Supporting Information

Supporting Information is available from the Wiley Online Library or from the author.

Conflict of Interest

The authors declare no conflict of interest.

Author Contributions

M.W.K. conceived the project and conducted all grafting experiments. Furthermore, he performed and interpreted all CA and SEM measurements. A.G. performed a significant part of the grafting reactions under supervision of M.W.K. during an internship. P.N. fitted and interpreted all XPS data. Furthermore, he proofread the manuscript. D.S. fabricated all titanium dioxide coated glass surfaces using special PVD techniques. I.G. facilitated the machinery required for the titanium dioxide coating process and contributed to the interpretation of results that were discussed in the current work. J.R. facilitated the machinery required for the XPS measurements, and contributed to the discussion of the results of the current project. R.H. facilitated the required preknowledge, work space, analytical support, and financial support that were required for this work.

[1] a) R. M. Donlan, *Clin. Infect. Dis.* **2001**, *33*, 1387; b) D. Pavithra, M. Doble, *Biomed. Mater.* **2008**, *3*, 034003; c) N. Cole, E. B. H. Hume, A. K. Vijay, P. Sankaridurg, N. Kumar, M. D. P. Willcox, *Invest. Ophthalmol. Visual Sci.* **2010**, *51*, 390; d) Y. Ohko, Y. Utsumi, C. Niwa, T. Tatsuma, K. Kobayakawa, Y. Satoh, Y. Kubota, A. Fujishima, *J. Biomed. Mater. Res.* **2001**, *58*, 97; e) K. Vasilev, J. Cook, H. J. Griesser, *Expert Rev. Med. Devices* **2009**, *6*, 553; f) M. D. P. Willcox, E. B. H. Hume, Y. Aliwarga, N. Kumar, N. Cole, *J. Appl. Microbiol.* **2008**, *105*, 1817; g) N. Wisniewski, M. Reichert, *Colloids Surf., B* **2000**, *18*, 197; h) C. Yang, G. L. Liang, K. M. Xu, P. Gao, B. Xu, *J. Mater. Sci.* **2009**, *44*, 1894; i) K. T. Meilert, D. Laub, J. Kiwi, *J. Mol. Catal. A: Chem.* **2005**, *237*, 101; j) J. Bozja, J. Sherrill, S. Michielsen, I. Stojiljkovic, *J. Polym. Sci., Part A: Polym. Chem.* **2003**, *41*, 2297; k) B. Meyer, *Int. Biodeterior. Biodegrad.* **2003**, *51*, 249; l) X. Li, Y. Xing, Y. Jiang, Y. Ding, W. Li, *Int. J. Food Sci. Technol.* **2009**, *44*, 2161; m) A. Conte, G. G. Buonocore, A. Bevilacqua, M. Sinigaglia, M. A. D. Nobile, *J. Food Prot.* **2006**, *69*, 866; n) E.-R. Kenawy, S. D. Worley, R. Broughton, *Biomacromolecules* **2007**, *8*, 1359; o) P. Asuri, S. S. Karajanagi, R. S. Kane, J. S. Dordick, *Small* **2007**, *3*, 50; p) D. M. Yebra, S. Kiil, K. Dam-Johansen, *Prog. Org. Coat.* **2004**, *50*, 75; q) L. D. Chambers, K. R. Stokes, F. C. Walsh, R. J. K. Wood, *Surf. Coat. Technol.* **2006**, *201*, 3642; r) H.-C. Flemming, *Appl. Microbiol. Biotechnol.* **2002**, *59*, 629.

[2] a) R. O. Darouiche, *N. Engl. J. Med.* **2004**, *350*, 1422; b) B. W. Trautner, R. O. Darouiche, *Am. J. Infect. Control* **2004**, *32*, 177; c) I. H. Jaffer, J. C. Fredenburgh, J. Hirsh, J. I. Weitz, *J. Thromb. Haemostasis* **2015**, *13*, S72.

[3] M. Hakim, I. Utama, B. Nugroho, A. Yusim, M. Baithal, I. Suastika, *IOP Conf. Ser.: Earth Environ. Sci.,* IOP, Ambon, Indonesia **2019**, *339*, 012037.

[4] I. B. Beech, J. Sunner, *Curr. Opin. Biotechnol.* **2004**, *15*, 181.

[5] S. Chen, L. Li, C. Zhao, J. Zheng, *Polymer* **2010**, *51*, 5283.

[6] L. Q. Xu, D. Pranantyo, J. B. Liu, K.-G. Neoh, E.-T. Kang, Y. X. Ng, S. L.-M. Teo, G. D. Fu, *RSC Adv.* **2014**, *4*, 32335.

[7] P. Petrov, G. Georgiev, D. Momekova, G. Momekov, C. B. Tsvetanov, *Polymer* **2010**, *51*, 2465.

[8] J. Telegdi, T. Rigó, J. Beczner, E. Kálmán, *Surf. Eng.* **2005**, *21*, 107.

[9] a) P. Bertrand, A. Jonas, A. Laschewsky, R. Legras, *Macromol. Rapid Commun.* **2000**, *21*, 319; b) C. Freij-Larsson, T. Nylander, P. Jannasch, B. Wesslén, *Biomaterials* **1996**, *17*, 2199.

[10] a) C. D. Bain, E. B. Troughton, Y. T. Tao, J. Evall, G. M. Whitesides, R. G. Nuzzo, *J. Am. Chem. Soc.* **1989**, *111*, 321; b) S. P. Pujari,

[11] L. Scheres, A. T. M. Marcelis, H. Zuilhof, *Angew. Chem., Int. Ed.* **2014**, *53*, 6322.

[11] H. Lee, S. M. Dellatore, W. M. Miller, P. B. Messersmith, *Science* **2007**, *318*, 426.

[12] J. H. Waite, *J. Exp. Biol.* **2017**, *220*, 517.

[13] J. H. Waite, M. L. Tanzer, *Science* **1981**, *212*, 1038.

[14] J. Saiz-Poseu, J. Mancebo-Aracil, F. Nador, F. Busqué, D. Ruiz-Molina, *Angew. Chem., Int. Ed.* **2019**, *58*, 696.

[15] H. Lee, N. F. Scherer, P. B. Messersmith, *Proc. Natl. Acad. Sci. USA* **2006**, *103*, 12999.

[16] S. M. D. Haeshin Lee, W. M. Miller, P. B. Messersmith, *Science* **2007**, *318*, 426.

[17] a) R. Batul, T. Tamanna, A. Khaliq, A. Yu, *Biomater. Sci.* **2017**, *5*, 1204; b) T. G. Kim, H. Lee, Y. Jang, T. G. Park, *Biomacromolecules* **2009**, *10*, 1532.

[18] Q. Wei, F. Zhang, J. Li, B. Li, C. Zhao, *Polym. Chem.* **2010**, *1*, 1430.

[19] Q. Wei, K. Achazi, H. Liebe, A. Schulz, P.-L. M. Noeske, I. Grunwald, R. Haag, *Angew. Chem., Int. Ed.* **2014**, *53*, 11650.

[20] a) M. W. Kulka, I. S. Donskyi, N. Wurzler, D. Salz, Ö. Özcan, W. E. S. Unger, R. Haag, *ACS Appl. Bio Mater.* **2019**, *2*, 5749; b) M. Li, C. Schlaich, M. W. Kulka, I. S. Donskyi, T. Schwerdtle, W. E. Unger, R. Haag, *J. Mater. Chem. B* **2019**, *7*, 3438.

[21] C. Schlaich, L. Yu, L. C. Camacho, Q. Wei, R. Haag, *Polym. Chem.* **2016**, *7*, 7446.

[22] a) K. Prime, G. Whitesides, *Science* **1991**, *252*, 1164; b) J. H. Lee, J. Kopecek, J. D. Andrade, *J. Biomed. Mater. Res.* **1989**, *23*, 351.

[23] S. Han, C. Kim, D. Kwon, *Polymer* **1997**, *38*, 317.

[24] A. Judge, K. McClintock, J. R. Phelps, I. MacLachlan, *Mol. Ther.* **2006**, *13*, 328.

[25] M. W. Kulka, I. S. Donskyi, N. Wurzler, D. Salz, Ö. Ozcan, W. E. S. Unger, R. Haag, *ACS Appl. Bio Mater.* **2019**, *2*, 5749.

[26] C. Siegers, M. Biesalski, R. Haag, *Chem. Eur. J.* **2004**, *10*, 2831.

[27] a) Q. Wei, S. Krysiak, K. Achazi, T. Becherer, P.-L. M. Noeske, F. Paulus, H. Liebe, I. Grunwald, J. Dernedde, A. Hartwig, T. Hugel, R. Haag, *Colloids Surf., B* **2014**, *122*, 684; b) T. B. Qiang Wei, R.-C. Mutihac, P.-L. M. Noeske, F. Paulus, R. Haag, I. Grunwald, *Biomacromolecules* **2014**, *15*, 3061.

[28] a) E. Moore, B. Delalat, R. Vasani, G. McPhee, H. Thissen, N. H. Voelcker, *ACS Appl. Mater. Interfaces* **2014**, *6*, 15243; b) M. Khan, W. T. S. Huck, *Macromolecules* **2003**, *36*, 5088.

[29] T. Weber, M. Bechthold, T. Winkler, J. Dauselt, A. Terfort, *Colloids Surf., B* **2013**, *111*, 360.

[30] Q. Wei, T. Becherer, P.-L. M. Noeske, I. Grunwald, R. Haag, *Adv. Mater.* **2014**, *26*, 2688.

[31] A. Sunder, R. Hanselmann, H. Frey, R. Mülhaupt, *Macromolecules* **1999**, *32*, 4240.

[32] P. Louette, F. Bodino, J.-J. Pireaux, *Surf. Sci. Spectra* **2005**, *12*, 38.

[33] C. Schlaich, L. Cuellar Camacho, L. Yu, K. Achazi, Q. Wei, R. Haag, *ACS Appl. Mater. Interfaces* **2016**, *8*, 29117.

[34] M. E. Lynge, R. van der Westen, A. Postma, B. Städler, *Nanoscale* **2011**, *3*, 4916.

2000931 (11 of 11)